University of Reading

School of Mathematics, Meteorology & Physics

The computation of spectral representations for evolution PDE

Sanita Vetra

August 2007

This dissertation is submitted to the Department of Mathematics in partial fulfillment of the requirements for the degree of Master of Science.

Acknowledgments

First, I would like to thank my supervisor Beatrice Pelloni for all the help she has provided, the patience answering all my questions and the endless enthusiasm and interest in the project. I also would like to thank the rest of the teaching staff in the maths department for all their support throughought the year. And many thanks to Sue Davis who has been like a second mum to all of us this year. Secondly, thanks to all my course mates for the interesting chats we have had in the room 107, the great times out and for the support they have given to me. It has been very enjoyable to go through

Abstract

In this dissertation we evaluate numerically the solution representations obtained from a recently developed Fokas integral method for solving boundary value problems for linear evolution PDEs. In particular, we consider the case of the linear KdV equation. The Fokas method is quite general and it is therefore of wider interest to assess its competitiveness for numerical purposes. Until now pseudospectral methods have been know to be the most accurate numerical scheme for smooth functions. In the work following, the linear KdV equation will be computed numerically using both a pseudospectral method and the dircet evaluation of the integral representation, and comparisons will be made between these two methods for accuracy and speed of the numerical computation.

Contents

1 Introduction

1

		4.2.1	Results for the linear KdV problems for $t 2[0; 2p]$	43
		4.2.2	Results for the linear KdV problems for $t 2 [0; 24p] \dots \dots \dots \dots \dots$	44
	4.3	Compa	rison between the methods	45
5	Non	linear Numerical Results 48		
	5.1	Pseudo	spectral method using the split-step method	48
		5.1.1	Non-linear step	49
		5.1.2	Linear step	51
		5.1.3	Numerical results from pseudospectral method	53
	5.2	Pseudo	spectral method and Fokas integral method using the split-step method \ldots .	53
6	Conclusions and Further Work			56
Bi	Sibliography 5			

Bibliography

List of Figures

1.1	The contour <i>C</i> corresponding to Jordan's Lemma.
2.1	The regions D^+ , D_1 , D_2 where $Re[i(k \ k^3)] < 0.$
3.1	Chebyshev points, projections onto x axis of equally spaced points on the unit circle
	with N = 27

;

 $t \ 2 \ [0; 10p]$, where w =

Chapter 1

Introduction

In this project we consider the analytical and numerical solutions of initial boundary value problems for evolution partial differential equations (PDEs) with constant coefficients, posed on a half line. These equations are of the form

$$q_t(x;t) + Tq(x;t) = 0; t > 0; x 2 [0;¥) (1.1)$$

where T is an x-differential operator. We prescribe initial data

 $q(x;0) = q_0(x);$ x 2[0;4];

where $q_0(x)$ is a given smooth function, such that $q(x;t) \neq 0$ as $x \neq 4$ and an appropriate number of boundary conditions are prescribed.

Equations of type (1.1) describe processes that are evolving in time from a given initial state. The simplest example is the heat or diffusion equation, $q_t = q_{xx}$, which models how heat diffuses starting from a given initial temperature.

The classical way of solving this type of problem is using a Fourier type transforms on the real line. For example, the heat equations on the half line with q(0;t) given is solved by the sine transform, while the same equation but with $q_x(0;t)$ given is solved by the cosine transform. Thus, the type of transform needed for a given initial boundary value problem is specified by the PDE, by the domain, and by the given boundary conditions. For simple boundary value problems there exists an algorithmic procedure for deriving the associated transform [9]. However, for many problems the classical transform method fails. For example, as we will see in *Chapter 2*, there does not exists a real fourier type transform for solving third order equations on the half line.

A new transform method was introduced by Fokas in 1997 [5], where the solution was found by rewriting the PDE as a Lax pair and then performing a simultaneous spectral analysis of it. Using this approach one can express the solution in the form of an integral for all linear and integrable non-

we consider the following given data,

$$\begin{cases} 8 \\ < q(x;0) = xe^{-ax} & a 2(0;1] \\ \vdots & q(0;t) = \sin(wt) & w 2 \mathbb{R}; \end{cases}$$
(1.7)

For the three linear cases a solution will be computed numerically both via the new Fokas method and by spectral methods, which will enable us to compare the two methods. In the case of non-linear KdV, the solution will be obtained using split step method where one step will compute solution using Fokas method and other using spectral method. This will be compared to the results obtained from purely spectral code. In *Chapter 3* an overview of the pseudospectral methods will be given. It will be shown in *Chapter 4* that the novel integral representations given by the new Fokas method are suitable for the numerical evaluation of the solution. This is possible, as using simple contour deformations in the complex k-plane, to obtain integrals involving integrants with strong decay for large k. [1] In Chapter 4 we look at the numerical results for the problems (1.3) - (1.5) and compare the results obtained from both methods for each of the problems. Lastly, in Chapter 5 we solve the problem (1.7) by pseudospectral methods using the Fourier split-step and give a motivation for combining the Fokas method for the linear part with pseudospectral method for the nonlinear part. All of the numerical schemes presented in this work are performed using Matlab. Codes, developed in this project, for the new Fokas integral method have been adopted from [11] and codes for pseudospectral methods have been adopted from [3]. It is possible that the codes' performance can be enhanced but this is not the focus of the present project.

1.1 Korteweg-de Vries (KdV) equation

The KdV equation is defined by,

$$q_t + q_x + qq_x + q_{XXX} = 0$$

and it was derived in 1895 by Korteweg and de Vries to describe long wave propagation on shallow water. It is an integrable, dispersive nonlinear evolution equation and it relates the amplitude of the wave and its change in space, with the change of the amplitude in time [3]. The spatial variable *x* is usually assumed to be real (so there is some decay at infinity) or on torus (so the data is periodic)

[17].

The intriguing property of the KdV equation is that under certain circumstances the dispersion and nonlinearity balance each other out, thus allowing the special solutions that travel without changing there shape. Korteweg and de Vries showed that the equation posed on the real line possesses a soliton solution, which takes the form

 $q(x;t) = 3c^2 \operatorname{sech}^2 \quad \frac{cx \quad c^3 t}{c^3 t}$

Chapter 2

The Fokas Spectral Transform Method for Linear Evolution PDEs on Half Line

In this project we study the linear KdV equation (2.4). Hence, we shall now use this as an example to describe the general method. The heat equation and Stokes first equations follow similarly and for Schrödinger equation and/or more detail on these and other problems the reader is referred to [1] - [3], [5], [6].

2.1 General Solution

Consider the linear KdV equation (2.4) posed on the half line,

$$q_t + q_x + q_{XXX} = 0; \quad x \ge [0; ¥):$$

To model an initial and boundary value problem, we need to supplement the equation with initial conditions and one boundary condition at x = 0. Hence, we always assume

$$q(x;0) = q_0(x)$$
(2.5)

and we shall specify boundary conditions below.

Using Fourier Transform we have

$$\hat{q}(k;t) = \int_0^{4} e^{-ikx} q(x;t) \, dx$$

then by integration by parts we obtain

$$q_{x}(k;t) = q(0;$$

We can define *t* transforms on the left boundary by

$$\tilde{g}_j(k;t) = \int_0^t e^{(ik - ik^3)s} \P^j_x q(0;s) \, ds; \qquad t > 0 \text{ for } j = 0, 1, 2$$
(2.10)

and

$$\tilde{g}(k;t) = \tilde{g}_2(k;t) + ik\tilde{g}_1(k;t) + (1 \quad k^2)\tilde{g}_0(k;t); \qquad k \ 2 \ \mathbb{R};$$
(2.11)

Thus, rearranging (2.8) we get expression for *x* transform of q(x; t),

$$\hat{q}(k;t) =$$

where $\hat{q}(k;0) = \int_0^4 \sin(kx) q(x;0) \, dx$.

Thus, the integral representation for the solution obtained via the sine transform in this case is fully defined in terms of the data of the problem. Note however, that (2.14) is not uniformly convergent as $x \neq 1$, so we cannot compute q(0;t) by just letting x = 0.

However, for the first Stokes equation (2.3) or the linear KdV this approach fails and it has been shown that for an odd number of spatial derivatives there are no *x*-transforms which could give a solution involving only known functions [7]. This is confirmed by the linear KdV for which the *x*-transform has the given solution (2.13) involving unknown functions.

The main difference between the new approach and the Fourier transform approach just obtained is to integrate along complex contours instead of the real line. i.e. *k* is no longer real but rather a complex variable. This allows the use of complex analytic techniques.

Using analyticity considerations, we obtain the integral representation in the form

$$q(x;t) = \frac{1}{2p} \int_{-\frac{1}{2}}^{\frac{1}{2}} e^{ikx} (ik-ik^3)t \, \hat{q}_0(k) \, dk + \frac{1}{2p} \int_{\P D_+} e^{ikx} (ik-ik^3)t \, \tilde{g}(k;t) \, dk;$$
(2.15)

where now $k \mathcal{2}\mathbb{C}$ and where $\P D_+$ is the contour in the upper half complex *k*-plane where the exponential $e^{i(k-k^3)}$ is purely oscillatory. The domain *D* is defined by

$$D = fk \ 2 \ \mathbb{C} : Re(ik \quad ik^3) \quad 0g; \qquad D = D \ \mathbb{C}$$

contour $\P D_+$, i.e. the integral along the rays $(-4; -1=^{p_{\overline{3}}}] [1=^{p_{\overline{3}}}] = 2$ can be deformed along the curves (in blue) shown in Fig.(2.1). These curves are the two branches of the curve *Re*(

and consider a simplified global relation,

$$(k^{2} \quad 1)\tilde{g}_{0}(k;t) = \tilde{g}_{2}(k;t) + ik\tilde{g}_{1}(k;t) + \hat{q}_{0}(k) \qquad Im(k) \quad 0:$$
(2.18)

We consider this relation for $k \ge \P D_+$, as this is the contour at which we need to characterise the unknown functions. Note that this contour is the boundary of the domain D_+ . Also, that the global relation is only well defined if Im(k) = 0. This is due to the fact that the term $\hat{q}_0(k)$

2.2.1 Dirichlet boundary condition

Let,

$$q(0;t) = f(t)$$
 (2.23)

for which our Fourier Transform is $\tilde{g}_0(k;t) = \int_0^t e^{(ik-ik^3)s} q(0;s) ds = \int_0^t e^{(ik-ik^3)s} f(s) ds$.

Here, we can express terms $\tilde{g}_1(k;t)$ and $\tilde{g}_2(k;t)$ in terms of $\tilde{g}_0(k \quad g \quad g_2(ik^3)$

Substituting (2.24) and (2.25) into (2.11) we have

$$\tilde{g}(k;t) = k^2 \tilde{g}_0(k;t) + \frac{n_1 \tilde{q}_0(n_2) - n_2 \tilde{q}_0(n_1)}{n_2 - n_1} + ik - \frac{k}{i} \tilde{g}_0(k;t) + \frac{\tilde{q}_0(n_2) - \tilde{q}_0(n_1)}{i(n_1 - n_2)} + (1 - k^2) \tilde{g}_0(k;t)$$

which simplifies to

$$\tilde{g}(k;t) = (1 \quad 3k^2)\tilde{g}_0(k;t) + \hat{q}_0(n_1)\frac{k \quad n_2}{n_2 \quad n_1} + \hat{q}_0(n_2)\frac{n_1 \quad k}{n_2 \quad n_1}$$
(2.26)

and substituting (2.26) into (2.15) gives

$$q(x;t) = \frac{1}{2p} \int_{-\frac{\pi}{2}}^{\frac{\pi}{2}} e^{ikx - (ik - ik^3)t} \hat{q}_0(k) dk + \frac{1}{2p} \int_{\frac{\pi}{2}} e^{ikx - (ik - ik^3)t} (1 - 3k^2) \tilde{g}_0(k;t) + \frac{1}{2p} \int_{\frac{\pi}{2}} e^{ikx - (ik - ik^3)t} \hat{q}_0(n_1) \frac{k - n_2}{n_2 - n_1} + \hat{q}_0(n_2) \frac{n_1 - k}{n_2 - n_1} dk$$

$$(2.27)$$

which is the solution to the linear KdV (2.4) subject to initial conditions (2.5) and Dirichlet boundary conditions (2.23).

Example 1: Linear KdV with Dirichlet BC and zero IC

Now we find a solution to the particular linear KdV problem with initial and boundary data defined as follows,

$$q(x;0) = 0$$
 (2.28)

$$q(0;t) = \sin(wt)$$
: (2.29)

Fourier Transforms of the initial condition is

$$\hat{q}_{0}(k) = \int_{0}^{4} e^{-ikx} q(x;0) dx$$

= 0 (2.30)

and of boundary condition is,

$$\tilde{g}_0(k;t) = \int_0^t e^{(ik-ik^3)s} q(0;s) \, ds$$

$$= \int_{0}^{t} e^{(ik - ik^{3})s} \sin(ws) \, ds$$

= $\frac{1}{w} \cos(ws) e^{(ik - ik^{3})s} \int_{0}^{t} + \frac{ik - ik^{3}}{w} \int_{0}^{t} e^{(ik - ik^{3})s} \cos(wt) \, ds$
= $\frac{1}{w} \cos(wt) e^{(ik - ik^{3})t} + \frac{1}{w} + \frac{ik - ik^{3}}{w} - \frac{1}{w} \sin(ws) e^{(ik - ik^{3})s} \int_{0}^{t} - \frac{ik - ik^{3}}{w} \tilde{g}_{0}(k;t) \, ds$

SO,

$$\tilde{g}_0(k;t) \quad \frac{w^2 + (ik - ik^3)^2}{w^2} \quad = \quad \frac{1}{w}\cos(wt)e^{(ik - ik^3)t} + \frac{1}{w} + \frac{ik - ik^3}{w^2}$$

The Fokas Spectral Transform Method for Linear Evolution PDEs on Half Line

Here, (2.21) - n₁² 1

$$q(x;0) = x^2 e^{-ax}; \quad a \ 2 \ \mathbb{R}^+$$
 (2.42)

$$q_x(0;t) = \sin(wt)$$
: (2.43)

Fourier Transforms of the initial condition is

$$\hat{q}_{0}(k) = \int_{0}^{4} e^{-ikx} q(x;0) dx = \int_{0}^{4} x^{2} e^{-(ik+a)x} dx$$

$$= \underbrace{\frac{e^{-(ik+a)x}}{(ik+a)} x^{2}}_{(ik+a)} + \frac{2}{(ik+a)} \int_{0}^{4} x e^{-(ik+a)x} dx$$

$$= \underbrace{\frac{e^{-(ik+a)x}}{(ik+a)} x}_{(ik+a)} + \frac{2}{(ik+a)^{2}} \int_{0}^{4} e^{-(ik+a)x} dx$$

$$= \frac{2}{(ik+a)^{2}} \frac{e^{-(ik+a)x}}{(ik+a)} = \frac{2}{(ik+a)^{3}}$$
(2.44)

and of the boundary condition is the same as for the case 1, but here it is $\tilde{g}_1(k;t)$ which is provided by given data,

$$\begin{split} \tilde{g}_{1}(k;t) &= \int_{0}^{t} e^{(ik-ik^{3})s} q_{x}(0;s) \, ds \\ &= \cdots \\ &= \frac{e^{(ik-ik^{3})t}}{2} - \frac{e^{-(ik-ik^{3})t} - e^{-iwt}}{(w-(k-k^{3}))} + \frac{e^{-(ik-ik^{3})t} - e^{iwt}}{(w+(k-k^{3}))} \end{split}$$
(2.45)

Thus, again substituting the equations for initial and boundary data (2.45) and (2.44) into the general solution (2.41) yields,

$$q(x;t) = \frac{1}{p} \int_{+}^{+} e^{ikx - (ik - ik^3)t} \frac{1}{(ik+a)^3} dk + (2.46) + \frac{1}{4p} \int_{\P D_+} e^{ikx} - 3ik - \frac{i}{k} - \frac{e^{-(ik - ik^3)t} - e^{-iwt}}{(w - (k - k^3))} + \frac{e^{-(ik - ik^3)t} - e^{iwt}}{(w + (k - k^3))} dk + + \frac{1}{2p} \int_{\P D_+} e^{ikx - (ik - ik^3)t} - \hat{q}_0(n_1) \frac{n_2^2 - k^2}{n_1^2 - n_2^2} + \hat{q}_0(n_2) \frac{k^2 - n_1^2}{n_1^2 - n_2^2} dk$$

integral representation to the linear KdV equation with Neumann boundary data,

$$q(x;t) = \frac{1}{p} \int_{=}^{=} e^{ikx} e^{ikx} (ik - ik^3)t \frac{1}{(ik+a)^3} dk +$$

Chapter 3

Pseudospectral Methods

Spectral methods were introduced in the 1970s and they have become widely popular for their accuracy and convergence speed when applied to smooth functions in comparison to the finite difference (FD) and finite element (FE) methods.

In this chapter we give an overview of pseudospectral methods, concentrating on the case of nonperiodic problems, in particular for third order equations.

The essential difference between spectral as opposed to finite difference/finite element approximations is that the latter approximates functions locally, using only the information available in some of N thus making it much more accurate than finite elements or finite difference methods, but also because of the high accuracy spectral methods are memory minimizing, too. Thus, if high accuracy

3. It should be fast to convert between coefficient[a_{k_i} $k = 0; ...; N_i$, and the values for the sum $u(x_i)$ at some set of node[x_i , $i = 0; ...; N_i$. It turns out that $u_N = I_N u$ is precisely the interpolant of u on the given node[. Thus, spectral metu 7[can also be de[cribed in term[of interpolation propertie[.

That is basis sets need to be easy to compute, have fast convergence and completenes[. The choice of the basis functions is determined by the type of problem at hand, for periodic functions trigonometric functions satisfy the above criteria and for non-periodic functions one resorts to using Chebyshev or Legendre polynomials; we will concentrate on Chebyshev polynomials referring the reader to [12] or [14] for background on other types of polynomials.

3.1 Non-periodic problems

Consider a non-periodic smooth function defined on [-1,1]. In general, when a smooth function is extended it becomes non-smooth and if trigonometric interpolation in equispaced points is used, then the above given criteria for $f_k(x)$ will not be satisfied. Thus, spectral accuracy will be lost and hence, the main reason for using spectral metu 7[.

Instead, we must replace trigonometric polynomials with algebraic polynomials,

$$p(x) = a_0 + a_1(x) + \dots + a_N(x)$$

on unevenly spaced points. We will use Chebyshev points, which are defined by

$$x_j = \cos \frac{jp}{N}$$
; $j = 0, 1, ..., N;$ (3.1)

and are the projections onto the interval [-1,1], of equispaced points along the unit circle in the complex plane, see Fig. 3.1. Chebyshev polynomials are defined a[

$$T_n(\cos q) = \cos(nq)$$
: (3.2)

We can see how the use of these points increases the accuracy of polynomial interpolant. For example, if we interpolate $u(x) = \frac{4}{5+128x^2}$ on a 21 point grid, then the maximum error on an equispaced grid is 72.4399, but using Chebyshev points the maximum error is only 0.014837. The difference in

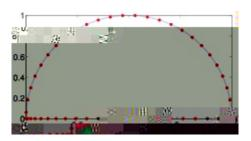


Figure 3.1: Chebyshev points, projections onto x axis of equally spaced points on the unit circle with N = 27.

easily seen in Fig. (3.2), where the interpolant on the left is oscillating near the ends of the interval (Gibbs phenomena see [10]). However, Chebyshev points approximate function u(x) very well. By increasing the number of grid points accuracy for equispaced points decreases exponentially with oscillations escalating, where as for Chebyshev points accuracy increases exponentially.

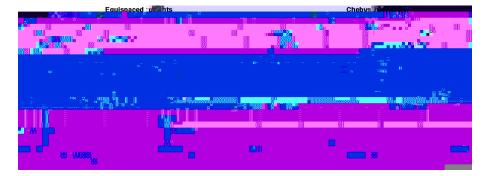


Figure 3.2: Interpolation of $u(x) = \frac{4}{5+128x^2}$ for equispaced and Chebyshev points.

3.1.1 Chebyshev differentiation matrices

Chebyshev points $x_j = \cos(jp=N)$ can be used to construct Chebyshev differentiation matrices, which then can be used to differentiate functions defined on these points. Now given a function u_j defined on Chebyshev points we obtain a discrete derivative w_j in two steps:

Let p(x) be the unique polynomial of degree N with $p(x_j) = u_j$, $0 \quad j \quad N$.

Set $W_j = p^{\ell}(x_j)$.

The differentiation operator is linear so it can be represented by multiplication by an (N+1) (N+1) matrix, which is denoted by D_N . Hence, we have

$$W = D_N u$$

where N is the number of grid points and can be odd or even positive integer.

Theorem 3.1.1 For each N = 1, let the rows and columns of the (N+1) = (N+1) Chebyshev spectral differentiation matrix D_N be indexed from 0 to N. The entries of this matrix are

$$(D_N)_{00} = \frac{2N^2 + 1}{6};$$
 $(D_N)_{NN} = \frac{2N^2 + 1}{6}$ (3.3)

$$(D_N)_{jj} = \frac{x_j}{2(1 - x_j^2)}, \qquad j = 1; ...; N \quad 1$$
 (3.4)

$$(D_N)_{ij} = \frac{c_i}{c_j} \frac{(1)^{i+j}}{x_i x_{j}}; \qquad i \notin j; \qquad i; j = 0; \dots; N$$
(3.5)

Ν

122j where

$$c_i = \begin{bmatrix} 8 \\ < \\ 222 \end{bmatrix}$$

We can truncate the spatial, x, domain, say at x = 40 as the solution decays rapidly and will be zero at this point. Hence, the problem now is defined on a finite, closed domain by,

$$u_t + u_x + u_{XXX} = 0 x 2 [0;40] (3.6)$$

with boundary conditions

$$u(0) = \sin(t)$$

 $u(40) = 0$ (3.7)
 $u_x(40) = 0$:

Note, that since now we have a bounded domain, we require three boundary conditions for the problem to be well-defined. That is, we have forced the solution and it's first derivative to be zero at the right boundary.

Now to make use of the Chebyshev differentiation matrix we need to transform spatial variable $x \ge [0;40]$ to $y \ge [-1;1]$. We use simple map for this

$$y = \frac{1}{20}x \quad 1$$

With the change in variable our problem (3.6) has changed too,

$$0 = u_t + y_x u_y + y_x^3 u_{yyy}$$
$$= u_t + \frac{1}{20} u_y +$$

this 'something else' to be polynomials as they are the easiest to compute.

So let

$$u(y;t) = g(y)q(y) + h(y);$$
(3.8)

where q(y) is a polynomial such that q(1) = 0 and g(y) and h(y) are smooth functions and h(y) satisfies the same boundary conditions as u.

Now at y = 1 we have that u(1) = h(1), but

$$u_y(1) = g(1)q_y(1) + h_y(1)$$

since u(y;t) and h(y) satisfy the same boundary conditions, then we require that g(1) = 0. The simplest function giving this is g(y) = y 1. Lastly we need to find h(y) such that $h(1) = h_y(1) = 0$ and $h(-1) = \sin(t)$,

$$h(y) = \frac{a+2c}{4}y^{2} + \frac{b}{2}ay + \frac{3b+a}{4}2c$$

$$= \frac{\sin(t)}{4}y^{2} + \frac{\sin(t)}{2}y + \frac{\sin(t)}{4}$$

$$= \sin(t) \quad \frac{y^{2}}{4} - \frac{y}{2} + \frac{1}{4} \quad : \qquad (3.9)$$

Hence, substituting above into (3.8)

$$u(y) = (y \quad 1)q(y) + \sin(t) \quad \frac{y^2}{4} \quad \frac{y}{2} + \frac{1}{4} \quad ; \tag{3.10}$$

and so first three derivatives of u(y; t) are

$$u_{y} = (y \ 1)q_{y} + q + \sin(t) \ \frac{y}{2} \ \frac{1}{2}$$
$$u_{yy} = (y \ 1)q_{yy} + 2q_{y} + \sin(t)\frac{1}{2}$$
$$u_{yyy} = (y \ 1)q_{yyy} + 3q_{yy}$$

Now, backward Euler formula is

$$\frac{u(t+Dt)}{Dt} \quad \frac{u(t)}{20} = \frac{u_y}{20} \frac{u_{yyy}}{8000}$$
$$= (y \quad 1)q_y + q + \sin(t) \quad \frac{y}{20}$$

3.2 Time-dependent problems

In general, the time coordinate is not treated spectrally. Discretising the spatial coordinate by a pseudospectral algorithm leaves us with a system of ODEs of the form $u_t = f(u; x; t)$, with u and f being vectors which can be marched forwards in time using some time stepping scheme like Backward Euler or Runge-Kutta. In principle, one sacrifices spectral accuracy in doing so, but in practice, small time steps with formulas of order two or higher often leave the global accuracy quite satisfactory. Marching with small time steps is much cheaper than computing the solution simultaneously over all space-time [12, 13].

We use backward Euler scheme in above polynomial trick method, which is applied to all linear problems in this project. Backward Euler scheme is of order O(Dt) and thus for it not to undermine the spectral accuracy we need to use small time steps. The fourth order Runge-Kutta scheme (RK4) has been used to obtain nonlinear numerical results in *Chapter 5*. The benefits of using RK4, a rather expensive do5 49(method,)-theris that it stable w0(Da⁴) arghestep0costepic dostepic date decay 390(do]TJ 0 -19.129 Td [(methot lits important that an accurate time stepping scheme is used, as otherwise the high spectral accuracy would be compromised. Backward Euler is much easier (and possibly cheaper) to implement, and if smaller time steps is not a problem, then this approach is preferred over the RK4 scheme for its

Chapter 4

Linear Numerical Results

In this chapter we consider the numerical solution of the linear KdV equation. In particular, we com-

(2.32) to the problem (1.3), given by

$$q(x;t) = \frac{1}{4p}$$

Here we use the analytic function,

$$k(\mathbf{q}) = i\mathbf{g}\sin(\mathbf{a} \quad i\mathbf{q}) \tag{4.1}$$

to map the points q onto the real line to a hyperbola type contours in complex *k*-plane [11]. Thus, once mapping is applied, the solution becomes

$$Q(x;t) = \frac{1}{4p} \int_{R} e^{ik(q)x} (1 \quad 3k(q)^{2}) \bigotimes_{\substack{\substack{a \in (k(q)-ik(q)^{3})t = e^{ikt} \\ \frac{(w \quad (k(q)-k(q)^{3})}{k(q)^{3})} \\ (??)}} \left\{ \frac{e^{-(ik(q)-ik(q)^{3})t} - e^{ikt}}{(w + (k(q)-k(q)^{3}))} \right\} \bigotimes_{\substack{\substack{a \in (k(q)-k(q)^{3})t = e^{ikt} \\ \frac{(w \quad (k(q)-k(q)^{3})}{k(q)^{3}} \\ (??)}}} \left\{ \frac{e^{-ik(q)-ik(q)^{3}}}{(w + (k(q)-k(q)^{3}))} \right\} \bigotimes_{\substack{\substack{a \in (k(q)-k(q)^{3})t = e^{ikt} \\ \frac{(w \quad (k$$

Hence, we want to deform $\P D_+$ to a contour for which we can expect Trefethen's results. For this we need the solution to be bounded and analytic in the shaded regions in the Figures (4.3), (4.6). Now e^{ikx} is analytic and decaying in \mathbb{C}^+ , $e^{-i(k-k^3)t}$ is analytic and decaying in the shaded regions in the Figures (4.3), (4.6) and e^{iwt} does not depend on *k* and so is analytic and decaying for fixed *t* but any *k* values. Lastly, we need to check if there are any singularities in the denominators of (??). For simplicity we take w = 1, then roots of $k^3 - k + 1 = 0$ are

$$k_0$$
 1:32472; k_1 0:662 + 0.562*i*; k_2 0:662 0:562*i* (4.3)

and roots of k^3 k 1 = 0 are,

$$k_0^{\ell} = k_0; \quad k_1^{\ell} = 0.662 + 0.562i; \quad k_2^{\ell} = 0.662 = 0.562i; \quad (4.4)$$

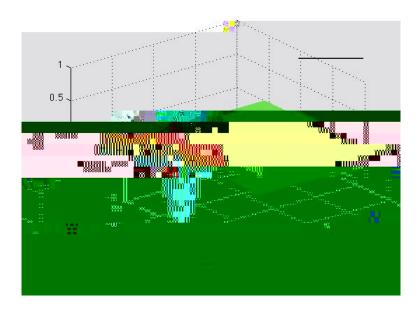
Thus, we can deform $\P D_+$ to any contour inside the shaded regions, if we avoid zeros of the denominators of (??).

Keeping this in mind we consider the following two possibilities as integration contour:

Hyperbola along ray p=12

The simplest case is to define $\P D_+$ on a hyperbola through the origin asymptotic to the rays p=12 and 11p=

Linear Numerical Results



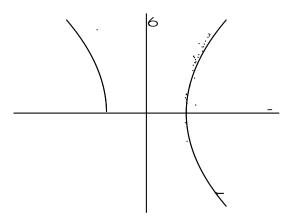
This mapping gives the following solution to the problem (1.3) on $x \ge 2[0/200]$; $t \ge 2[0/2p]$,

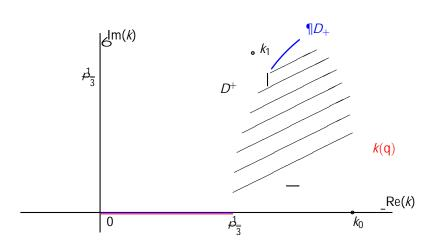
Figure 4.4: Numerical solution for the linear KdV by simple mapping along p=12 ray

Shifted hyperbola along the ray $p\!=\!\!6$

.

A more involved but equally simple case is to take k(q) = q for 0 Re(k) $1 = \frac{\rho_{\overline{3}}}{3}$ and for $Re(k) > 1 = \frac{\rho_{\overline{3}}}{3}$ apply mapping $k(q) = igsin(a iq) ilm(k(1 = \frac{\rho_{\overline{3}}}{3}))$, see Fig. (4.5).





have singularities. However, the shift of the imaginary part in the second case introduces numerical instability in the solution and as a result the solution possesses periodic waves, see Fig. (4.7). This can be solved by finer discretisation in q, but that means more computation time. Hence, we give the upper hand to the first method, and will use it for all of the numerical computations here.

Next is the question: how far along the q

```
for kk = 0:N
    theta = kk h;
    k = i ga sin(alpha i theta);
    q = 1/(4 pi) exp(ikx)(1 3k^2). ...
        ((exp( i(k k^3)t) exp( iwt))/(w (k k^3))+...
        (exp( i(k k^3)t) exp( iwt))/(w+(k k^3)));
    term = real(q gamma cos(alpha i theta));
    sol = sol+term;
    if k == 0; sol = 0.5sol; end
end
sol = (2h)sol;
```

Exponentials e^{ikt} and e^{-ikt} can be computed once outside the loop as their value does not depend on k and terms can be grouped for $e^{-i(k-k^3)t}$, for faster computations.

4.1.3 Results for the linear KdV problems for t 2 [0/2p]

Here we present the numerical results of the thr

4.1.4 Results for the linear KdV problems for t 2 [0;15p]

To see how the initial wave is dispersing we need to compute the solution for larger *t*. **Numerical solution of Example 1**

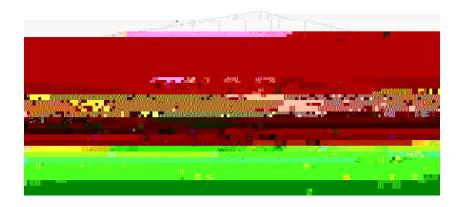
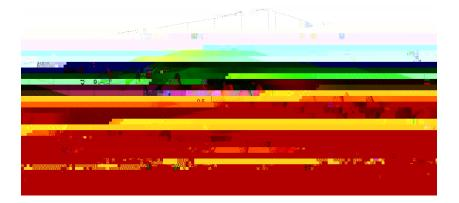


Figure 4.12: Numerical solution of the linear KdV with q(x;0) = 0 and $q(0;t) = \sin(wt)$ for $t \ge 2$ [0;10p], where w = 1 using the new Fokas transform method, with a = p=12, g = 0.53



Numerical solution of Example 2

Figure 4.13: Numerical solution of the linear KdV with $q(x;0) = xe^{-ax}$ and $q(0;t) = \sin(wt)$ for $t \ge 2[0;10p]$, where w = 1 using the new Fokas transform method, with a = p = 12, g = 0.53

terms involving the unknown function q(y) can be grouped together (all matrices) as in (3.11),

$$L = \frac{(y-1)}{Dt}D_N^0 + \frac{(y-1)}{20}D_N^1 + \frac{D_N^0}{20} + \frac{(y-1)D_N^3 + 3D_N^2}{8000}$$

and all the left over terms are known (all vectors), as in (3.12)

$$f(y) = \frac{u(t)}{Dt} \quad \frac{1}{Dt}\sin(t+Dt) \quad \frac{y^2}{4} \quad \frac{y}{2} + \frac{1}{4} \quad \frac{\sin(t)}{20} \quad \frac{y}{2} \quad \frac{1}{2} \quad :$$

Hence, we have a simple matrix problem to solve (3.13), given by

$$Lq(y) = f(y)$$

To do this, we exploit the simple Matlab matrix solver q(y) = Lnf(y).

The error for spectral methods is exponentially decreasing, i.e. it is of order $O(h^N)$ or $O(1=N^N)$, as we use N = 128 in all the computations, then for all of the spectral methods the error introduced by spectral discretisation is

However, the backward Euler method is of order

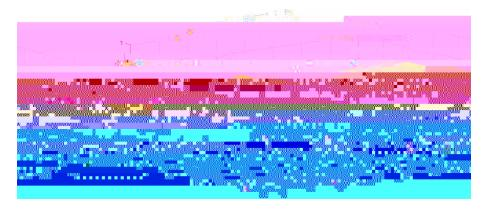
4.2.1 Results for the linear KdV problems for t 2 [0; 2p]

Here we present the numerical results of the three linear KdV problems as set out in *Chapter 1* and for which integral representations were found in *Chapter 2*.

Numerical solution of Example 1



Figure 4.15: Numerical solution of the linear KdV with q(x;0) = 0 and q(0;t) = sin(wt) for $t \ge [0;2p]$, with w = 1.



Numerical solution of Example 2

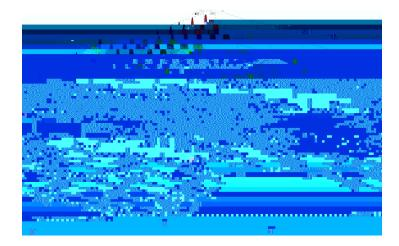
Figure 4.16: Numerical solution of the linear KdV with $q(x;0) = xe^{-ax}$ and $q(0;t) = \sin(wt)$ for $t \ge 2[0;2p]$, with w = 1

4.2.2 Results for the linear KdV problems for t 2 [0/24p]

To see how the initial wave is dispersing we need to compute the solution for larger *t*. **Numerical solution of Example 1**

	0.5~
2, 1, 1, 1, 1, 1, 1, 1, 1, 1, 1, 1, 1, 1,	
-27. Martin Bland Handler Martin Program (1998)	

Figure 4.17: Numerical solution of the linear KdV with q(x;0) = 0 and q(0;t) = sin(wt) for $t \ge [0;24p]$, with w = 1



Numerical solution of Example 2

Figure 4.18: Numerical solution of the linear KdV with $q(x;0) = xe^{-ax}$ and $q(0;t) = \sin(wt)$ for $t \ge 2[0;24p]$, with w = 1

4.3 Comparison between the methods

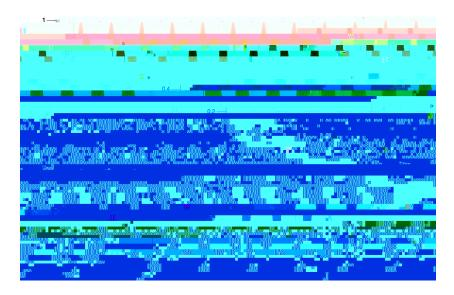
To compare the two methods, since the pseudospectral method can only be used in conjunction with Chebyshev points, then we can either run the code for the Fokas method on Chebyshev points, which are mapped into *x* space, i.e. $y \ge [-1/1] ! x \ge [0/40]$, or on an equally spaced *x* grid and with small Dx which then leaves us to match the nearest points. We measure the absolute difference between the two solution matrices to gain the error estimate. The two methods at most differed by 0.04, and that could be lowered provided the Fokas integral is evaluated on much finer grid. Hence, the two methods are approaching the same solution. Even though this does not provided an estimate of the error in either of the methods or codes, it still gives a verification that methods are computing correctly the solution.

We have not computed the Example 3, defined in (1.5), using pseudospectral methods as it is requires a method other than the polynomial trick for us to apply the Chebyshev differentiation matrix and it is out of the scope of this project. However, this illustrates the benefits of using the Fokas integral solutions as not only the method is general to all linear PDEs of type (1.1), but also the numerical method is exactly the same for all of these problems, one only needs to change the integral obtained (as in *Chapter 2*) and put it in the code. When using other methods we are forced to use different methods depending on the problem for computing the solution.

Max *t* vavlauleue

Linear Numerical Results

Solutions from both of methods, as expected show decrease in hight of the main solitary wave. This process is slow, especially if energy in initial condition is large. We can see this especially well in Fig. (4.19).



Chapter 5

Nonlinear Numerical Results

As the numerical computation has proved to be so easy to implement and to such high accuracy, it is just natural to try to compute the nonlinear KdV next. In this chapter we are interested in looking at the nonlinear KdV equation defined in (1.6),

q

and hence, the boundary data for this part is

$$q(1;t) = 0:$$

Hence, we have

$$u_t(y;t) = (1 \quad y)q(y;t)_t$$

$$u_y(y;t) = q(y;t) + (1 \quad y)q_y(y;t);$$

and in terms of q(y; t), (5.3) is given by

$$(1 \quad y)q_t(y;t) + \frac{1}{20}(1 \quad y)q(y;t) [\quad q(y;t) + (1 \quad y)q_y(y;t)] = 0$$

Rearranging above we obtain,

$$q_{t}(y;t) = \frac{1}{20}q^{2}(y;t) + \frac{1}{20}q(y;t)q_{y}(y;t)(1 \ y)$$

= $\frac{1}{20}q^{2}(y;t) + \frac{1}{40}q^{2}(y;t)y(1 \ y)$. (5.5)

Given an initial condition $u(y_j; 0)$, $0 \neq N$, then in terms of q(y; t) from (5.4), initial condition becomes

$$q(y_j;0) = \frac{u(y_j;0)}{(1-y_j)}:$$
(5.6)

We use the fourth order Runge Kutta scheme, given by,

$$q_{n+1} = q_n + \frac{1}{6} \left(d_1 + 2(d_2 + d_3) + d_4 \right)$$
(5.7)

where

$$d_{1} = \frac{Dt}{2} \qquad \frac{1}{20} q_{n}^{2}(y;t) + \frac{1}{40} [q_{n}(y;t)]_{y}^{2}(1 \quad y)$$

$$d_{2} = \frac{Dt}{2} \qquad \frac{1}{20} q_{n}(y;t) + \frac{1}{2} d_{1}^{2} + \frac{1}{40} q_{n}(y;t) + \frac{1}{2} d_{1}^{2} \frac{q_{1}(y;t)}{y}$$

$$d_{3} = \frac{Dt}{2} \qquad \frac{1}{20} q_{n}(y;t) + \frac{1}{2} d_{2}^{2} + \frac{1}{40} q_{n}(y;t) + \frac{1}{2} d_{2}^{2} \frac{q_{1}(y;t)}{y}$$

$$d_{4} = \frac{Dt}{2} \qquad \frac{1}{20} [q_{n}(y;t) + d_{3}]^{2} + \frac{1}{40} [q_{n}(y;t) + d_{3}]_{y}^{2}(1 \quad y)$$

Nonlinear Numerical Results

the same polynomial method as in *Chapter 3* and it is readily seen that we obtain the same linear system as in (3.13) but with half a time step, i.e. now instead of (3.11) we have

$$L = \frac{2}{Dt}(y - 1)D_N^0 + \frac{(y - 1)}{20}D_N^1 + \frac{D^0}{20} + \frac{(y - 1)}{8000}D_N^3 + \frac{3D_N^2}{8000}$$
(5.11)

and instead of (3.12) we have

$$f(y) = \frac{2}{Dt}u(t) \quad \frac{2}{Dt}\sin(t+Dt) \quad \frac{y^2}{4} \quad \frac{y}{2} + \frac{1}{4} \qquad \frac{\sin(t+Dt=2)}{20} \quad \frac{y}{2} \quad \frac{1}{2} \quad (5.12)$$

Hence, the method can be summarized as follows,

set initial data u_0 set initial time t = 0set final time tMaxset Dtcompute number of plots nplots = tMax=dt

for i = 1: *nplots*

- 1. Advance the nonlinear part $u_t + uu_x = 0$ by t + Dt = 2 from time t to time t + Dt = 2. If i = 1 use given initial data u_0 , else use data from linear part obtained at i = 1.
- 2. Advance the linear part $u_t + u_x + u_{xxx} = 0$ by t + Dt = 2 from time t + Dt = 2 to time t + Dt. Initial data is always the solution from the nonlinear part.

end

Nonlinear Numerical Results

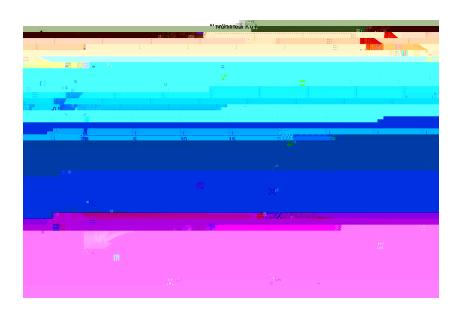


Figure 5.2: Comparison between linear and nonlinear KdV solution with $u(x;0) = xe^{-x}$ and u(0;t) = sin(t), for $x \ge [0;40]$, $t \ge [0;8]$

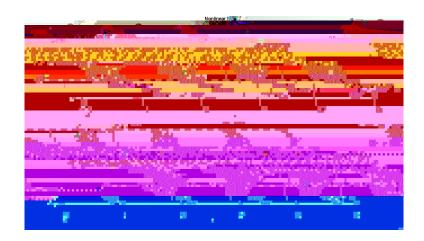


Figure 5.4: Comparison between linear and nonlinear KdV solution with $u(x;0) = x^2 e^{-x}$ and $u(0;t) = \sin(t)$, for $x \ge [0;40]$, $t \ge [0;8p]$.

the split step method.

This would involve solving the nonlinear part, $u_t + uu_x = 0$, as above using the Chebyshev differentiation matrix and a time stepping scheme like RK4. Then, the linear part, $u_t + u_x + u_{xxx} = 0$, would use the solution obtained from the Fokas integral method. Since, both linear and nonlinear parts have to "communicate" with each other, that is the linear part needs to use the solution from the nonlinear part and vice versa, we cannot use the code developed for the Fokas method as is. If we would use the numerical integration on the linear part as we have done in *Chapter 4* then the "communication" would be only one way and the linear part would never know what the nonlinear part does. What we require is to take the solution from the nonlinear part as an initial data for the linear part and evaluate it at k, μ_1 and μ_2 (e.g. for Dirichlet case \hat{q}_0 in (2.27)). Note, that since we cannot solve now for the initial data analytically we compute it using the FFT (Fast Fourier Transform) and the IFFT(Inverse Fast Fourier Transform) pair.

The difficulty is in the computation via FFT of the transform of the new initial condition not only for *k* real, but also at the other points needed in order to evaluate the integral representation. This work is in progress, as it presents a more serious challenge than we originally envisaged. This method should produce more accurate results than the pure pseudospectral method and its computation speed should also improve, especially for larger domains.

Chapter 6

Conclusions and Further Work

In this chapter we summarize the work carried out in this dissertation. We will discus the main results of the work carried out here and refer the reader to the relevant chapters. We will also indicate the areas for possible further research in the topic.

The aim of this dissertation was to compare the numerical results of the recently developed Fokas integral method for solving boundary value problems for linear and integrable nonlinear PDEs in two variables and the well known pseudospectral methods. The Fokas integral method produces the exact solution in the integral form. This only leaves us to do the numerical integration, which is much easier to do than use any other methods developed until now for the numerical computation of linear evolutionary PDEs on the half line. Moreover, it also proves to be much more accurate.

The theory of the Fokas integral method was developed in *Chapter 2* and we used the linear KdV equation to illustrate the method. Even though the method was explained only in terms of the linear KdV, exactly the same method applies to ALL linear evolutionary PDEs. Because of this, the method is of great importance as it provides a generalized way of solving such equations, rather than needing to resort to a specific transform (and in many cases not being able to solve the problem at all). Moreover, in comparison to solutions obtained using classical Fourier transforms, the integral representation obtained from the Fokas method is uniformly convergent at the boundaries and it is spectrally decomposed. In *Chapter 2*, we found the general solutions for both Dirichlet and Neu-

Thus, the conclusion is that the new Fokas integral method is a first general method which can be applied to all the linear evolutionary PDEs. It produces an analytic integral representation of the solution around a contour in the complex plane. Using simple numerical integration method, it is extremely easy to implement the method numerically. It is more accurate than the pseudospectral methods, and if accuracy is an issue, the Fokas method is also faster too (as currently implemented).

Because of the ease of implementation of the linear method it would be very useful to apply this approach for the nonlinear case too. Thus, in *Chapter 5* we first described the split step method for solving the nonlinear KdV equation using pseudospectral methods as currently one of the most accurate schemes for this equation. Then we give an outlay of how the solution from the Fokas method for the linear KdV could be used in the second step to give us a hybrid method, one which is half pseudospectral and half numerical integration of the solutions from the Fokas method. We have not been able to develop or implement this idea in this project because of the time constraints. However, it would be an interesting path to explore, as if implemented successfully, it would provide a more accurate solution than the purely pseudospectral method and the speed of computation should improve too, as the step size in time would not need to be so small.

Bibliography

- [1] Flyer N., Fokas A.S. (2007), "A new Transform Method for the Numerical Integration of Evolution PDEs", Proc. Roy. Soc. A, (preprint)
- [2] Fokas A.S. (2002), "A new Transform Method for Evolution Partial Differential Equations", IMA Journal of Applied Mathematics, 67:559-590.
- [3] Chilton, D. (Jul. 2006),

- [10] Gottlieb D., Shu C. W. (1997), "The Gibbs Phenomenon and its Resolution", SIAM Review, 39:644668.
- [11] Flyer N., Personal communication
- [12] Boyd J.P. (2001), "Chebyshev and Fourier Spectral Methods", 2nd edition, Dover Publications Inc. (UK)
- [13] Trefethen L.N. (2002), "Spectral Methods in Matlab", SIAM (USA)
- [14] Fornberg B. (1998), "A Practical Guide to Pseudospectral Methods", Cambridge University Press (UK)
- [15] Iserles A. (1996), "A First Course in the Numerical Analysis of Differential Equations", Cambridge Texts in Applied Mathematics, Cambridge University Press
- [16] Wolfram Research Inc. (2007), "Numerical Solution of Partial Differential Equations", Online Mathematica Tutorial, URL: http://reference.wolfram.com/mathematica/tutorial/NDSolvePDE.html
- [17] Colliander J., Keel M., Staffilani G., Takaoka H., Tao T., "Equations of Korteweg de Vries type", URL: http://www.math.ucla.edu/ tao/Dispersive/kdv.html, accessed on 05/07/2007
- [18] Davenport C. M. (2006), "The General Analytical Solution for the Korteweg- de Vries Equation", URL: http://home.usit.net/ cmdaven/korteweg.htm, accessed on 11/08/2007